USASP
US ASSOCIATION FOR THE STUDY OF PAIN

PUBLISHED BY
ELSEVIER

The Journal of Pain, Vol 25, No. 6 (June), 2024: 104457
Available online at www.jpain.org and www.sciencedirect.com

Reduced Gray Matter Volume and Cortical Thickness in Patients With Small-Fiber Neuropathy

Sebastian Scheliga,[*] Maike F. Dohrn,[†] Ute Habel,[*,‡] Angelika Lampert,[§] Roman Rolke,[¶] Annette Lischka,[‖] Noortje van den Braak,[†] Marc Spehr,[**] Han-Gue Jo,[††] and Thilo Kellermann[*,‡]

[*]*Department of Psychiatry, Psychotherapy and Psychosomatics, Medical Faculty RWTH Aachen University, Aachen, Germany,* [†]*Department of Neurology, Medical Faculty RWTH Aachen University, Aachen, Germany,* [‡]*Institute of Neuroscience and Medicine: JARA-Institute Brain Structure Function Relationship (INM 10), Research Center Jülich, Jülich, Germany,* [§]*Institute of Neurophysiology, Medical Faculty RWTH Aachen University, Aachen, Germany,* [¶]*Department of Palliative Medicine, Medical Faculty RWTH Aachen University, Aachen, Germany,* [‖]*Institute for Human Genetics and Genomic Medicine, Medical Faculty RWTH Aachen University, Aachen, Germany,* [**]*Department of Chemosensation, RWTH Aachen University, Institute for Biology II, Aachen, Germany,* [††]*School of Computer Information and Communication Engineering, Kunsan National University, Gunsan, South Korea*

Abstract: **Small-fiber neuropathy (SFN) is defined by degeneration or dysfunction of peripheral sensory nerve endings. Central correlates have been identified on the level of gray matter volume (GMV) and cortical thickness (CT) changes. However, across SFN etiologies knowledge about a common structural brain signature is still lacking. Therefore, we recruited 26 SFN patients and 25 age- and sex-matched healthy controls to conduct voxel-based- and surface-based morphometry. Across all patients, we found reduced GMV in widespread frontal regions, left caudate, insula and superior parietal lobule. Surface-based morphometry analysis revealed reduced CT in the right precentral gyrus of SFN patients. In a region-based approach, patients had reduced GMV in the left caudate. Since pathogenic *gain-of-function* variants in voltage-gated sodium channels (Nav) have been associated with SFN pathophysiology, we explored brain morphological patterns in a homogenous subsample of patients carrying rare heterozygous missense variants. Whole brain- and region-based approaches revealed GMV reductions in the bilateral caudate for Nav variant carriers. Further research is needed to analyze the specific role of Nav variants for structural brain alterations. Together, we conclude that SFN patients have specific GMV and CT alterations, potentially forming potential new central biomarkers for this condition. Our results might help to better understand underlying or compensatory mechanisms of chronic pain perception in the future.**

Perspective: ***This study reveals structural brain changes in small-fiber neuropathy (SFN) patients, particularly in frontal regions, caudate, insula, and parietal lobule. Notably, individuals with SFN and specific Nav variants exhibit bilateral caudate abnormalities. These findings may serve as potential central biomarkers for SFN and provide insights into chronic pain perception mechanisms.***

Key words: *Small-fiber neuropathy, Gray matter volume, Cortical thickness, Voxel-based morphometry, Surface-based morphometry*

Received June 1, 2023; Received in revised form December 8, 2023; Accepted January 2, 2024
Supplementary data accompanying this article are available online at www.jpain.org and www.sciencedirect.com.
Address reprint requests to Sebastian Scheliga, Department of Psychiatry, Psychotherapy and Psychosomatics Medical Faculty RWTH Aachen University, Pauwelsstraße 30, 52074 Aachen, Germany.
E-mail: sscheliga@ukaachen.de
1526-5900/$36.00

https://doi.org/10.1016/j.jpain.2024.01.001

Small-fiber neuropathy (SFN) is a complex neurological disorder that primarily affects small unmyelinated nerve fibers in the peripheral nervous system. SFN is clinically characterized by neuropathic pain and autonomic symptoms (eg, pupil abnormalities, impotence, dry eyes or mouth early satiety and gastric fullness, abnormal sweating, hot flushes, and/or cardiac palpitations, skin decolouration).[1,2] An epidemiological investigation conducted on SFN has taken place in the Netherlands. This study revealed a consistent minimum annual incidence rate of 12 cases per 100,000 residents, accompanied by enduring and persistent symptoms.[3] SFN patients report a significantly reduced quality of life, pointing toward unmet needs in the diagnostic and therapeutic workup and lack of knowledge. Altogether, the diagnosis does not only cause a major burden for patients, but also for the health care and socioeconomic system. What is known is that both dysfunction and degeneration of thinly myelinated Aδ-fibers and unmyelinated C-fibers can cause SFN symptoms.[2] Therefore, the assessment of intraepidermal nerve fiber density (IENFD) and quantitative sensory testing (QST) is crucial to confirm the diagnosis.[1,4-6]

SFN has traditionally been considered as a disorder of the peripheral nervous system.[7,8] Only few magnetic resonance imaging (MRI) studies have analyzed potential SFN effects on the brain.[9-11] Upon skin nerve degeneration, a core feature of SFN,[9,10] white matter connectivity, functional connectivity, and gray matter volume (GMV) were reduced in pain-related brain regions. Specifically, reduced GMV and cortical thickness (CT) have been reported in patients with diabetic (painful and painless) peripheral neuropathy. Here, regional GMV loss was identified, for example, in thalamus, caudate nucleus, cingulate cortex, insula, and precentral regions, while CT was reduced in frontal regions.[12-14] To date, it remains unclear whether corresponding effects are reproducible in a non-diabetic SFN patient population.

Gain-of-function variants in genes encoding the voltage-gated sodium channel (Nav) subunits Nav1.7, Nav1.8, and Nav1.9 (*SCN9A*, *SCN10A*, and *SCN11A* respectively) have recently been discovered in SFN patients.[15-17] In SFN, *gain-of-function* Nav variants are associated with several phenotypes with presence or absence of autonomic symptoms and different pain distributions[2] meaning not all SFN patients suffer from pain but may have sensory symptoms such as numbness or coldness.[18] These Nav channels are predominantly expressed in peripheral neurons and have been associated with several pain disorders.[19,16,17,20,21-23] Alterations that enhance the function of SCN9A result in profound neuropathic pain, while *loss-of-function* mutations lead to insensitivity toward pain.[19] Research indicates that there exists an underlying cause for SFN, wherein the presence of mutated *gain-of-function* sodium channels in axons of small peripheral nerves could potentially lead to the degeneration of these fibers.[16] Also, studies on peripheral neuropathy showed that *gain-of-function* mutations may enhance the channel's response to depolarization and causing a hyperexcitability in dorsal root ganglion neurons. This suggest *gain-of-function* mutations contribute to peripheral neuropathy.[17] However, less is known about central pain markers in SFN patients carrying Nav gene variants. Here, we set out to investigate voxel-based- and surface-based morphometry (VBM/SBM) in SFN patients and healthy subjects, adjusting for age, sex, and total intracranial volume (TIV).

We included patients with idiopathic SFN (meaning that no specific etiology has been identified yet) and hypothesized that SFN can be characterized by a common brain morphologic signature that has the potential to be a clinical SFN marker.

Additionally, we conducted explorative VBM- and SBM analyses on a patient subsample with heterozygous missense variants in *SCN9A*, *SCN10A*, and *SCN11A*. Here, we asked whether genetic alterations in ion channel subtypes correlate with structural changes of the brain. Based on previous literature, we expected reduced GMV[24-27] and CT[28,29] in brain regions involved in pain processing across SFN patients. To examine the clinical relevance of morphological alterations, we correlated neural findings with clinical parameters.

Methods

Participants

The study sample comprised 51 subjects in total, 26 SFN patients and 25 healthy controls (HC), who were all examined at the University Hospital Aachen, Rheinisch-Westfälische Technische Hochschule (RWTH) Aachen University, Germany, after obtaining written informed consent. The study has been approved by the local institutional review board (EK215-19) and conformed with the Declaration of Helsinki.

All patients were examined by the same, trained physicians. The SFN diagnosis was based on a typical patient history with neuropathic pain and additional sensory and/or autonomic symptoms as well as on clinical signs of small-fiber impairment (pinprick and thermal sensory loss and/or allodynia and/or hyperalgesia), with distributions consistent of peripheral neuropathy (length or non-length dependent). Additionally, at least one of the following criteria had to apply for study inclusion: evidence of small fiber dysfunction by quantitative sensory testing (Deutscher Forschungsverbund Neuropathischer Schmerz, DFNS protocol),[30-32] or evidence of small-fiber degeneration on histological examination, namely reduction of IENFD on a skin punch biopsy obtained at distal legs).[1] All patients underwent detailed neurological assessments,[30] by which the presence or absence of spontaneous pain (eg, thermal hyperalgesia and mechanical allodynia), and paresthesias or dysesthesias were recorded by a neurologist based on symptom descriptions. Patients also received nerve conduction studies to exclude large-fiber neuropathy. To eliminate the concern of possible central nervous system involvement of concomitant systematic diseases, patients with any clinical evidence of brain or spinal cord disorders were excluded.[9,10] Additionally, we excluded patients with neuropathies caused by diabetes mellitus, alcoholism,

Table 1. Participant Demographic and Clinical Data

	Healthy controls	*SFN patients*	*P-value*
N (m/f)	25 (12/13)	26 (11/15)	.781
Age[a]	41.04 (18.53)	45.31 (10.77)	.320
GM[a] (cm^3)	690.64 (92.59)	667.88 (67.76)	.320
WM[a] (cm^3)	537.04 (79.10)	537.00 (64.98)	.998
CSF[a] (cm^3)	320.52 (80.72)	332.12 (62.04)	.567
TIV[a] (cm^3)	1548.12 (187.45)	1537.19 (160.95)	.824
Thickness[a] (mm)	2.73 (.16)	2.71 (.10)	.482
Symptom duration (years)[a]	–	7.84 (4.88)	–
IENFD	–	4.01 (2.15)	–
CDT[a b] (test)	.43 (.28)	.57 (.23)	.100
CDT[a b] (control)	.10 (.23)	.49 (.32)	< .001
WDT[a b] (test)	.67 (.29)	.83 (.25)	.047
WDT[a b] (control)	.34 (.24)	.46 (.27)	.102
CPT[a b] (test)	10.61 (10.36)	11.72 (8.23)	.689
CPT[a b] (control)	10.46 (9.37)	12.77 (7.89)	.372
HPT[a b] (test)	46.08 (2.53)	45.32 (3.47)	.397
HPT[a b] (control)	45.71 (3.31)	41.98 (6.18)	.014
painDETECT	–	13.84 (8.02)	–
NRS	–	3.33 (2.08)	–

Abbreviations: m, male; f, female; GM, gray matter; WM; white matter; CSF, cerebrospinal fluid; TIV, total intracranial volume; IENFD, intraepidermal nerve fiber density; CDT, cold detection threshold; WDT, warm detection threshold; CPT, cold-pain threshold; HPT, heat-pain threshold; NRS, Numeric Rating Scale NOTE. [a] Mean (Standard deviation), [b]Logarithmically transformed QST thresholds are shown for test- and control area, respectively. The values for the healthy subjects were taken from a sex-, age-, and region-matched reference sample.

vitamin B12 deficiency, or chemotherapy. Moreover, we collected further information about symptom onset (illness duration) and applied the painDETECT questionnaire[33,34] and the Numerical Rating Scale (NRS) for pain[35-37] to characterize patients' subjective pain experience. We only included patients with idiopathic SFN. Idiopathic SFN" means that despite extensive diagnostic research, no underlying cause was found. Following a standardized protocol, we analyzed peripheral blood cell counts, glycated hemoglobin (HbA1c), carbohydrate deficient transferrin, vitamin B12, folic acid, creatinine, thyroid stimulating hormone, anti-nuclear antibodies, anti-neutrophil cytoplasmic antibodies, anti-citrullinated protein antibodies, rheumatoid factor, and creatine kinase. Additionally, to measuring the IENFD, histological assessments of skin biopsies included specific staining for inflammatory cell infiltrates and amyloid deposits. Participants were considered "idiopathic SFN patients" whenever all the above mentioned screening was inconclusive and SFN diagnosis confirmed. For all participants, demographics and clinical data can be found in Table 1. A binary sex definition ('sex assigned at birth') was used to categorize participants as male or female. Concerning the participants' racial background, only white (Caucasian) people attended in the control group. In the patient cohort, one Black- and 25 Caucasian individuals were assessed. Additional information on the patients' medication status is provided in the Supplementary Material (Table S1).

Within the patient sample, 9 subjects carried a rare heterozygous sodium channel missense variant, identified by whole exome sequencing. In short, DNA isolated from peripheral blood samples was sequenced on a NextSeq500 Sequencer with 2 × 75 cycles on a high-output flow cell (Illumina, San Diego, CA) using a probe-based capture method to enrich the target regions (Integrated DNA Technologies, Coraville, IA, or Nextera Rapid Capture Exome [version 1.2]; Illumina). Alignment to the reference genome (hg38) and variant calling were performed using an in-house pipeline based on SeqMule (http://seqmule.openbioinformatics.org/en/latest). Variant analysis and prioritization were performed using Kggseq software (http://pmglab.top/kggseq/). Out of the 9 identified subjects, 4 patients had a rare variant in the *SCN11A* gene (encoding Nav1.9), 3 patients carried a rare variant in the *SCN10A* gene (Nav1.8), and 3 patients had a rare *SCN9A* variant (Nav1.7). Of note, one subject carried a rare variant both in *SCN9A* and *SCN10A*, respectively. All variants were formally classified as variants of uncertain significance (ACMG criteria).[38] Further description on these genetic variants can be found in the supplement (Table S2).

MRI Acquisition

For imaging, we used a Siemens 3-Tesla MRI scanner (Prisma Magnetom). For each participant, we acquired anatomical brain scans by using a T1-weighted 3D sagittal magnetization-prepared rapid gradient echo sequence using the following parameters: 176 slices, repetition time = 200 ms, echo time = 3.03 ms, slice thickness = 1 mm, in plane resolution of 1 ×1 mm^2. Further we manually inspected the images for artefacts and image quality in general.

Volume-Based Processing and Analysis

We applied VBM to assess differences in gray matter volume between SFN patients and HC subjects. VBM comprises different processing steps: tissue segmentation, spatial registration, adjustments for volume changes due to the registration, and convolution with a Gaussian Kernel (spatial smoothing).[39] We used SPM12 (www.fil.ion.ucl.ac.uk), and the CAT12 toolbox (https://neuro-jena.github.io/cat/) to conduct VBM analyses.[40] For the VBM analyses, we preprocessed structural images with default settings of the CAT12 toolbox incorporating a correction for bias-field inhomogeneities, segmentation into gray matter, white matter, and cerebrospinal fluid. These 3 tissue components were obtained to calculate the overall tissue volume and TIV for each subject. This step was followed by spatial normalization to the DARTEL template in Montreal Neurological Institute (MNI) space. Finally, gray matter data were smoothed using an 8 mm full-width-half-maximum isotropic kernel.[41,42] After preprocessing, we used the CAT12 toolbox-function 'check sample homogeneity' to identify scans with poor image quality. For none of the images we found abnormalities so that none of the subjects had to be excluded from the statistical analyses.

For all VBM analyses, we used the CAT12 toolbox. In the main VBM analysis, we first calculated a general

linear model (GLM, t-contrast with 2 samples) to compare the GMV between SFN patients (n = 26) and the control group (n = 25). Age, sex, and TIV might be linked to (ie, not orthogonal to) the effects of interest[39] and were therefore included as covariates. The factor 'group' was considered as effect of interest comprising 2 levels, that is, HC subjects and SFN patients. For all whole brain VBM analyses, we set a cluster-defining threshold of $P < .001$ uncorrected. Due to the relatively small sample size and previous VBM studies that suggested GMV alterations may occur in chronic pain[43,24,27,44] and in neuropathic pain conditions particularly,[26,45] we were prompted to conduct whole brain analyses with a liberal threshold. However, we decided to additionally report, which of these clusters would also survive an false discovery rate (FDR)-correction at the cluster level of $P < .05$.

In addition to that, we calculated a region-based approach. Therein, for each subject regional measurements were automatically calculated by conducting the pipeline for voxel-based processing. Based on the Neuromorphometrics atlas (http://www.neuromorphometrics.com/) available in the toolbox, volumetric measures (ie, GMV) were calculated for each region in native space. Neuromorphometrics is an anatomical atlas based on multiple subjects. It was built using manual tracing on anatomical MRI from 30 healthy subjects. It is composed of 140 regions cortical and subcortical structures. We applied the same contrasts from the VBM analysis in order to identify GMV group differences that may manifest in certain regions included in the atlas. By using the region-based approach, we aim to validate the clusters identified from voxel-based analyses. After conducting the region-based approach, results were corrected for multiple comparisons by controlling the FDR,[46] using a threshold of $P < .001$.

Surface-Based Processing and Analysis

Besides GMV analysis, we also conducted surface-based processing following the procedure described by Gaser and colleagues.[39] Here, we used a fully automated method implemented in CAT12 to estimate CT and the central surface of hemispheres based on the projection-based thickness method.[47] Thereby, partial volume information, sulcal blurring, and sulcal asymmetries without explicit sulcus reconstruction were handled. Following this step, anatomically incorrect connections between sulci or gyri were repaired by using spherical harmonics.[48] After this topological correction, surface refinement was applied resulting in the final central, pial, and white matter surface meshes. Finally, with the FreeSurfer thickness metric, pial, and white matter surfaces were used to refine the initial CT estimate.[49,50] Individual central surfaces were then registered to the respective hemisphere from FreeSurfer *FsAverage* template. Doing so, central surfaces were spherically inflated with minimal distortions.[51] We used the 2D-version of the DARTEL approach to create one-to-one mapping between the folding patterns of the individual and the template spheres. After surface creation and surface registration, the images were smoothed with a 15 mm full-width-half-maximum Gaussian kernel.[39]

SBM was applied to investigate CT. Thereby, the measure of CT captures the width of the gray matter ribbon as the distance between its inner and outer boundary at thousands of points.[39] We conducted the main SBM analysis to assess differences in CT between SFN patients and HC. Comparably to the VBM analysis, we again calculated a GLM (t-contrast with 2 samples). The factor group was considered as effect of interest, while age and sex were included as covariates. Since CT is not closely linked to brain volume,[52] we did not include TIV as a covariate. For all SBM analyses, we set a cluster-defining threshold of $P < .001$ uncorrected. We further performed a surface-focusing region-based approach implemented in CAT12. Therein, a cortical surface parcellation[53] was supplied on the *FsAverage* surface that can be mapped to the individual surfaces by using the spherical registration parameters. CT was then calculated for each region in native space.[39] Results were corrected for multiple comparisons (FDR, $P < .001$).

In VBM and SBM, respectively, we used different brain structure analysis pipelines (whole brain and region-based approaches) in order to test whether identified voxel clusters from whole brain analysis represent a robust finding that can be validated by region-based analysis.

Exploratory Structural Analyses in Patients With Nav Variants

We further conducted 3 explorative VBM- and region-based analyses (volume-focusing) as well as 3 SBM- and region-based analyses (surface-focusing), respectively. Thereby, we first compared SFN patients carrying rare Nav variants (n = 9) with HC. Afterward, we analyzed differences between controls and patients without genetic variants (n = 17). We also compared the 2 patient subgroups to assess potential CT and GMV differences between patients with- and without Nav variants. For each VBM/SBM analysis a cluster-defining threshold of $P < .001$ uncorrected was set. For each region-based analysis, we used an FDR-corrected threshold of $P < .001$. Notably, this subsample was very small. Therefore, these analyses must be treated as a pilot assessment. The results must be interpreted with caution and replication by larger samples is needed.

Exploratory Partial Correlation Analyses

Finally, for all regions showing significant GMV differences between groups in the VBM whole brain analysis, the respective values were extracted, and correlated with the following clinical parameters: IENFD, illness duration, painDETECT score,[33,34] NRS score,[35] cold detection threshold (CDT), warm detection threshold (WDT), cold-pain threshold (CPT), and heat-pain threshold (HPT) (Quantitative Sensory Testing, QST

thresholds were taken from the patient's painful test area and control area, respectively).[31,32] In some patients, values of clinical parameters were not completely available resulting in varying sample sizes for correlation analyses: IENFD (n = 21), symptom duration (n = 25), NRS (n = 22), painDETECT (n = 25), CDT (test) (n = 23), CDT (control) (n = 23), WDT (test) (n = 23), WDT (control) (n = 23), CPT (test) (n = 23), CPT (control) (n = 23), HPT (test) (n = 23), HPT (control) (n = 23). In total, 12 clinical measures were correlated with GMV values from 4 brain regions, respectively, resulting in n = 48 tests. We further correlated GMV values of the 4 brain regions among each other (n = 12 tests) and we calculated correlations among the clinical parameters (n = 132 tests). We used Pearson's partial correlation analysis implemented in SPSS 27 controlling for age, sex, and TIV as covariates. The significance threshold was set at $P < .05$. Bonferroni correction was used to adjust for multiple testing across all the tests (N = 192).

Sensory Profiles in SFN Patients

A short form of the initial QST paradigm[31,32] was conducted containing 4 (CDT, WDT, CPT, HPT) instead of typical 13 parameters. QST was performed including a short demonstration of each test at a practice area until subjects understood the test procedure. For the correlation analyses, we used z-transformed QST values for CDT, WDT, CPT, and HPT. Here, we calculated z-values for each of the logarithmically transformed (for CDT and WDT) or QST raw data (for CPT, HPT) using the following term: $Z = (mean^{patient} — mean^{controls})/SD^{controls}$.[31] To calculate the z-profile for each patient, we used reference data from 23 healthy control subjects who were matched for age, sex, and body region. We used unpaired t-tests to assess differences in CDT, WDT, CPT, and HPT between SFN patients and healthy reference subjects (threshold at $P < .05$).

Automated Regional Behavioral Analyses

We aimed to functionally characterize the significant clusters that we received from the main VBM analysis (cluster-defining threshold of $P < .001$ uncorrected). Therefore, we used the BrainMap database (http://www.brainmap.org/)[54] to link the clusters with functional properties. In the database, we focused on the meta-category 'Behavioral domain' comprising 5 primary domains (Action, Cognition, Emotion, Interoception, and Perception) with 51 behavioral subcategories.[55,56] Each significant cluster revealed by VBM analysis was considered to create volumes of interest (VOIs). During automated behavioral analyses, the share of coordinates within these VOIs was calculated and compared with the share expected if coordinates were not uniformly distributed.[56] This procedure was performed for each behavioral sub-domain (for an overview of the sub-categories see the paper 47 and 22) to test whether these fractions differ. Here, large differences point to a behavioral association. Note that only behavioral sub-categories with positive z-scores of ≥3.0 are considered significant. Multiple comparisons were addressed by using a binomial test ($P < .05$) with Bonferroni correction implemented in the Brain map software.[56]

Data Availability

The data from this study are available on request from the corresponding author. The data are not publicly available due to their containing information that could compromise the participant's privacy.

Results

Sociodemographic and Clinical Variables

Between HC and SFN patients, there were no significant differences for the following variables: sex, age, total amount of gray- and white matter, respectively, cerebrospinal fluid, TIV, and total amount of cortical thickness. Concerning thermal thresholds from QST, patient's sensory profile and comparison with HC can be found in Section 3.5.1. Patients' data on IENFD can be found in the Supplementary Material (Table S3).

VBM Analyses

For the main VBM analysis, we accessed GMV differences between HC and SFN patients. Thereby, we identified several brain regions that showed significant GMV reductions in SFN patients compared to HC. These regions included the bilateral superior frontal gyrus (SFG), middle frontal gyrus (MFG), left caudate nucleus (caudate), insula, right medial superior frontal gyrus (mSFG), superior parietal lobule (SPL), and inferior frontal gyrus (IFG). Four of these regions also survived an FDR-corrected threshold of $P < .05$ at the cluster level, namely left SFG ($P = .015$), right mSFG ($P = .015$), right SPL ($P = .010$) and left caudate ($P = .007$). Volumes of these regions can be found in the supplement (Table S4). In the patient group, we found significantly larger GMV in the left precuneus and Raphe's nuclei (Table 2, Fig 1).

Region-Based Analyses (VBM)

For the region-based approach, we applied the same contrasts from the VBM analysis in order to identify regions showing GMV differences between HC and SFN patients (FDR, $P < .001$). Here, the first region-based analysis revealed one significant region showing significantly larger GMV in the control group, that is, the left caudate ($T = 3.633$, $P = .0004$). The reversed contrast yielded no region showing significantly larger GMV in the patient group.

SBM Analyses

For the main SBM analysis, we compared CT between HC and SFN patients. Reduced CT for SFN patients

Table 2. VBM: Significant Clusters for the Main Effect of Group (HC vs all SFN Patients)

Region	k	Peak MNI coordinates			Peak T-value*
		x	y	z	
Healthy controls > SFN patients					
L SFG	747	-27	2	54	5.48
R mSFG	719	15	48	45	5.16
R SPL	932	28	-75	51	4.87
L caudate	1144	-8	8	15	4.36
R MFG	119	30	33	34	4.21
L insula	44	-44	3	-6	3.76
R mSFG	33	12	58	21	3.57
R SFG	21	20	68	20	3.50
L MFG	8	-34	48	16	3.42
R IFG	4	54	20	2	3.34
R MFG	5	33	58	2	3.33
L insula	1	-42	14	-8	3.29
SFN patients > Healthy controls					
L precuneus	181	-10	-42	58	4.22
Raphe	1	0	-28	-15	3.28

Abbreviations: R, right; L, left; SFG, superior frontal gyrus; mSFG, medial superior frontal gyrus; SPL, superior parietal lobule; caudate, caudate nucleus; MFG, middle frontal gyrus; IFG, inferior frontal gyrus; Raphe, raphes nuclei.
NOTE. Extent threshold k = 0 voxels.
*Height threshold T = 3.277 ($P < .001$, uncorrected).

emerged in the right precentral gyrus (PreCG) (Table S5, Fig 2). There was no brain region with increased CT in patients.

Region-Based Analyses (SBM)

Besides to SBM whole brain analysis, we further conducted surface-based region-based analyses. Similar to the procedure for volume-based region-based approach, we used the same contrasts from the SBM analyses to assess differences in CT between the groups (FDR, $P < .001$). We did not find significant group differences between HC and SFN patients.

Exploratory Structural Analyses in Patients With Nav Variants

Explorative VBM Analyses

In the first out of 3 explorative VBM analyses, we compared HC (n = 25) with SFN patients carrying genetic Nav variants (n = 9). In Nav-patients, we identified significant GMV reductions in the bilateral caudate, left MFG, middle temporal gyrus (MTG), right superior occipital gyrus (SOG), and thalamus. Additionally, the second contrast yielded larger GMV in the left MTG cluster for Nav-patients compared to controls (Table 3). Considering significant regions for FDR correction at the cluster level, only the left caudate ($P = .018$), revealed from the first contrast, survived the more conservative threshold of $P < .05$ FDR-corrected at cluster level.

Next, we conducted the second explorative VBM analysis. Here, we compared HC (n = 25) and SFN patients that did not carry rare genetic Nav variants (n = 17). Compared to HC subjects, we identified significant GMV reductions in left SFG, thalamus, right MTG, SPL, mSFG, and MFG for the patient group. Furthermore, we found larger GMV for the patients in the left precuneus and right SOG (Table 4).

For the third explorative VBM analysis, we compared GMV between SFN patients with- and without genetic Nav variants. Here, the analysis did not reveal significant findings.

Explorative region-based analyses (VBM). We performed the region-based approach to compare HC subjects and patients with Nav variants (FDR, $P < .001$). Thereby, we identified 2 regions in the left- (T = 3.836, $P = .0003$) and right caudate (T = 3.494, $P = .001$) with

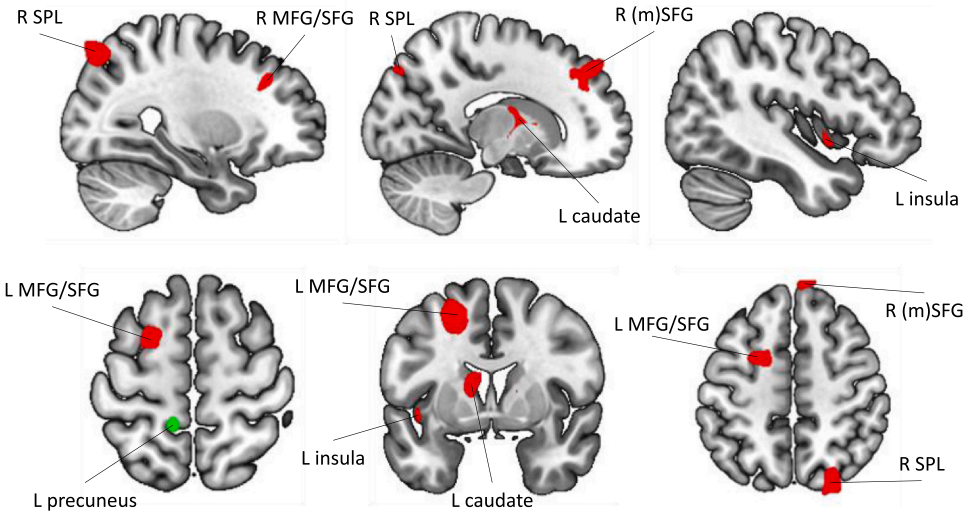

Figure 1. Differences in GMV between healthy controls and SFN patients. Displayed are brain regions showing reduced GMV (red) and increased GMV (green) in the patient group compared to HC. GMV was decreased for bilateral superior frontal gyrus (SFG), middle frontal gyrus (MFG), left caudate nucleus (caudate), insula, right medial superior frontal gyrus (mSFG), superior parietal lobule (SPL), and inferior frontal gyrus (IFG). The GMV for left precuneus and Raphe's nuclei was increased. All brain maps were thresholded at $P < .001$ at the voxel level (uncorrected).

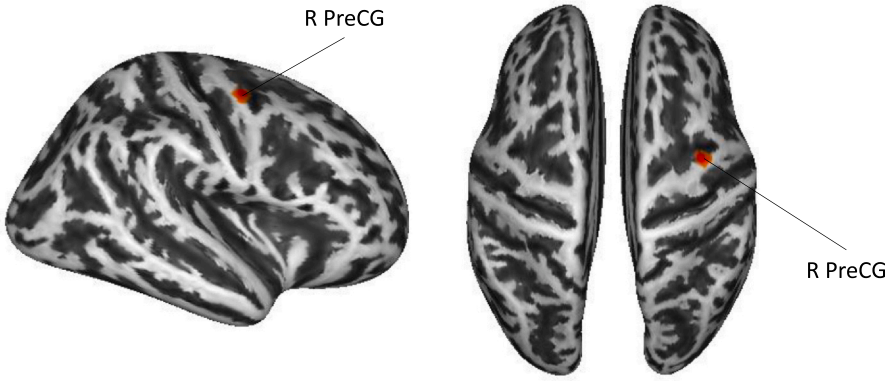

Figure 2. Differences in cortical thickness (CT) between healthy controls and SFN patients. Brain regions showing reduced CT in the patient group compared to HC are shown in red. CT was decreased for the right precentral gyrus (PreCG).

significantly larger GMV in the control group compared to patients with Nav variants. Neither the region-based analyses for the comparison between HC and patients without Nav variants nor for the comparison between patients with- and without variants yielded a significant finding.

Explorative SBM Analyses

Comparing HC and patients with Nav variants, we identified reduced CT for patients in the right PreCG and the right occipital pole (OP). Further, patients showed increased CT in left SPL, IPL, and right middle occipital sulcus and lunate sulcus (Table S6). Assessing CT differences between HC and patients without Nav variants, we found reduced CT for the patients in the right PreCG, while there was increased CT in medial occipital-temporal gyrus (Table S7). Finally, comparing SFN patients with and without Nav variants, we found that patients without genetic variants had increased CT in left medial occipital-temporal gyrus and right inferior parietal sulcus (Table S8).

Explorative region-based analyses (SBM). Only region-based analyses for the comparison of HC and SFN patients with Nav variants revealed a significant finding. The analysis yielded significantly increased CT in middle occipital sulcus and lunate sulcus for the patients (T = 3.505, $P = .001$). No further region-based analysis revealed significant group differences.

Correlation Analysis

To test whether our imaging findings can be linked to clinical parameters in the patient sample, a partial correlation analysis was performed. To concentrate on the most robust findings for the correlation analyses, we selected the 4 significant regions from the main VBM analysis (HC vs SFN patients) that survived FDR cluster level correction. Hence, we extracted the respective

Table 3. VBM: Significant Clusters for the Main Effect of Group (HC vs SFN Patients With Nav Variants)

Region	k	Peak MNI coordinates			Peak T-value*
		x	y	z	
Healthy controls > SFN patients with Nav variants					
L MFG	67	-26	3	58	4.45
L caudate	833	-6	18	9	4.38
R caudate	295	18	-8	16	3.98
R SOG	17	21	-81	39	3.66
L MFG	14	-32	54	18	3.63
R thalamus	12	20	-24	2	3.47
R caudate	1	20	-21	21	3.41
L MTG	1	-50	-42	-12	3.40
SFN patients with Nav variants > Healthy controls					
L MTG	144	-51	-26	-14	4.17

Abbreviations: R, right; L, left; MFG, middle frontal gyrus; caudate, caudate nucleus; SOG, superior occipital gyrus; MTG, middle temporal gyrus.
NOTE. Extent threshold k = 0 voxels.
*Height threshold T = 3.396 ($P < .001$, uncorrected).

Table 4. VBM: Significant Clusters for the Main Effect of Group (HC vs SFN Patients Without Nav Variants)

Region	k	Peak MNI coordinates			Peak T-value*
		x	y	z	
Healthy controls > SFN patients without Nav variants					
R MTG	339	56	-70	18	4.91
R SPL	661	27	-74	52	4.87
L SFG	499	-27	2	52	4.79
R mSFG	390	14	48	45	4.68
R MFG	49	30	33	34	3.87
R SPL	8	18	-58	52	3.67
R mSFG	56	12	57	20	3.63
L thalamus	2	-15	-3	9	3.33
SFN patients without Nav variants > Healthy controls					
L precuneus	122	-10	-42	58	4.27
R SOG	41	16	-88	32	3.89

Abbreviations: R, right; L, left; MTG, middle temporal gyrus; SPL, superior parietal lobule; SFG, superior frontal gyrus; mSFG, medial superior frontal gyrus; MFG, middle frontal gyrus; SOG, superior occipital gyrus.
NOTE. Extent threshold k = 0 voxels.
*Height threshold T = 3.325 ($P < .001$, uncorrected).

GMV values from the Neuromorphometrics atlas for the following 4 regions: left caudate, SFG, right mSFG, and SPL. Thereafter, the GMV-value of each region was correlated with eight z-transformed QST subscales (CDT, WDT, CPT, and HPT for both test- and control area), IENFD, illness duration, painDETECT score, and NRS score. Pearson's partial correlation analysis was conducted, controlling for age, sex, and TIV as covariates. Notably, since none of the SBM results survived FDR correction, correlation analysis was conducted for the VBM findings only.

None of the correlations survived Bonferroni correction for multiple testing. However, some significant results were found for the uncorrected correlations. Therefore, the uncorrected results has been added to the supplement (Table S9). Since GMV reduction in the caudate nucleus was found in both whole brain approach and region-based approach this result can be seen as the main finding of the study. Therefore, we reported the significant uncorrected correlations for the caudate only. For the left caudate, we observed significant inverse correlations with CPT (test) ($r = -.465$, $P = .039$), CPT (control) ($r = -.483$, $P = .031$), HPT (control) ($r = -.497$, $P = .026$), and a significant inverse correlation with IENFD ($r = -.468$, $P = .050$).

Sensory Profiles in Patients with SFN

We calculated t-tests to analyze differences in CDT, WDT, CPT, and HPT between SFN patients and controls. Compared with age-, sex-, and area-matched healthy subjects, SFN patients showed a significant cold hypoesthesia (CDT control) ($P < .001$), warm hypoesthesia (WDT test) ($P = .047$), and heat hyperalgesia (HPT control) ($P = .014$). Z-score sensory profiles are depicted in Fig 3.

Behavioral Associations with Regional VOIs

We defined 12 regional VOIs based on significant clusters (cluster-defining threshold of $P < .001$ uncorrected) from the main VBM analysis and performed automated behavioral analysis to determine functional profiles for the regions with GMV reductions in patients with SFN. For left SFG, analyses revealed significant associations with the behavioral domain Cognition. That is, with sub-categories Reasoning ($z = 3.728$) and Working Memory ($z = 3.137$). Further, left caudate was significantly associated with the behavioral domain Emotion, that is, with the subcategory Reward/Gain ($z = 5.966$).

For the remaining ten regions, we did not find any significant associations with behavioral domains. However, from our perspective it is worth mentioning that 7 VOIs in the frontal lobe and insula were slightly associated with the Inhibition subcategory from the Action domain ($z > 1.3$, see Table S10 in supplement). A complete list comprising each region and the respective peak z-values is presented in the supplement (Table S10).

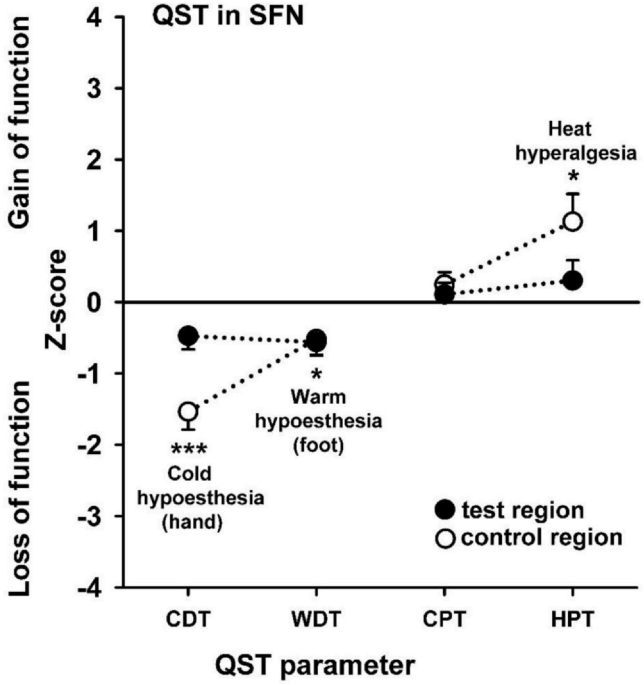

Figure 3. Quantitative sensory profiles. SFN patients had increased thermal detection thresholds indicating a loss of function for cold detection threshold (CDT) and warm detection threshold (WDT). Heat-hyperalgesia was found for the heat-pain threshold (HPT). Test region was mainly the foot, control region mainly hands. Asterisks denote levels of significance: *$P < .05$, ***$P < .001$.

Discussion

SFN is a disorder that affects not only peripheral nerves, but also brain structure. We found several GMV and CT changes in SFN patients. Most prominently, we identified a volume reduction in the left caudate that was evident for both voxel-based and region-based approaches. Automated behavioral analyses revealed an association between caudate and the behavioral category Reward, pointing to deficits in reward-processing. We observed reduced GMV in bilateral caudate for patients with rare genetic Nav variants but not for patients without such variants. It is an interesting finding that decreased bilateral GMV in the caudate can be found in patients carrying rare Nav missense variants. This would be consistent with the concept that persistently increased peripheral nociceptive input may lead to a possibly initially functional and then secondarily morphological decline in brain performance that is more pronounced in Nav variant carriers. Apart from the observed changes in the caudate, we identified GMV reductions in frontal areas, left insula, and right parietal lobule. Further, we used SBM to assess CT differences between patients and controls. We found reduced CT in right PReCG for the patients. Our findings point to GMV and CT reductions in SFN that may reflect a characteristic feature of the disorder.

We identified reduced GMV in the left caudate for SFN patients. GMV reductions in patients were assessed based on the voxel-based approach using a rather liberal cluster-defining threshold of $P < .001$ uncorrected.

GMV reduction in the left caudate also survived a designated correction method for multiple testing ($P < .001$, FDR) in the region-based approach. The caudate was the only region that we could identify with both approaches, whole brain- and region-based analysis pointing to the most robust finding. Thus, this converging evidence for the left caudate in region- and voxel-based analyses represent the key finding of GMV reduction in patients with SFN. Decreased caudate GMV has been reported for several pain conditions.[57-60] Behavioral analysis revealed a significant association between left caudate and the behavioral domain Emotion, suggesting a role for the caudate in reward processing. Reward and pain processing interact in overlapping brain systems and these systems may change with chronic pain.[61] A previous study reported impaired reward responsiveness in chronic pain patients accompanied by reduced GMV within the reward system.[62] Liu and colleagues[63] concluded chronic pain may reduce reward-seeking 'wanting-behaviors'. Reduced caudate GMV may reflect impaired reward processing and motivational deficits in chronic pain. Since activation of reward-related brain circuits have been discussed to reflect relief from the affective component of chronic pain,[64] GMV reduction in left caudate may hold potential for a biomarker that may be a target for new therapeutics. This patient cohort has been in-depth phenotyped and known causes of neuropathy excluded. That means on the one hand, that findings might be relatively specific, but on the other hand, further studies are needed to extrapolate our conclusions to the broader (acquired) SFN cohort.

In explorative VBM analyses, we found reduced GMV in bilateral caudate for patients carrying genetic missense variants, but not for patients without variants. This finding was supported by region-based analysis revealing reduced GMV in bilateral caudate for Nav-carriers compared to HC. We did not find similar effects in patients lacking such variants. This finding suggests that GMV reduction might be especially pronounced in *SCN9A*, *SCN10A*, and *SCN11A* genes. A previous fMRI study on erythromelalgia has shown that pathogenic variants in *SCN9A* were associated with activation of pain areas suggesting *gain-of-function* variants of peripheral ion channels might impact brain activity.[65] *Gain-of-function* variants in Nav channels produce hyperexcitability in dorsal root ganglion neurons[15] and inferior parietal sulcus-cell derived sensory neurons from patients.[66-68] It might be possible that enhanced firing of these neurons causing frequent nociceptive input negatively affect brain structures involved in pain suppression, for example, caudate.[69-71] These results need to be interpreted with caution since explorative VBM analyses were based on only 9 patients with Nav variants. We are aware that this subsample is very small. Therefore, these analyzes must be treated as a pilot study. The results must be interpreted with caution and replicated by larger samples. Disease causing variants have to be discriminated from disease-contributing variants and variants of uncertain significance.[72,73] Studies postulated that the frequency of specific variants is low in SFN and that these variants may be considered as risk factors, contributing to rather than causing disease.[2] The specific pathogenic significance of these variants remain uncertain and needs to be determined.

We found an inverse caudate GMV correlation with CPT and HPT, respectively. Smaller caudate volume was associated with lower temperature changes from neutral baseline needed to be perceived as painful, which is consistent with heat-hyperalgesia in the patient group, with sensory profiles reflecting C- and Aδ-fiber overactivity. Previous findings pointed to decreased caudate activation after painful thermal stimulation in patients with neuropathic pain.[74] Frequent nociceptive processing might lead to lower activations in the caudate associated with pain suppression.[69-71] We assume that decreased reactivity following nociceptive input might reflect insufficient pain suppression. We assume that decreased caudate volume might accompany decreased functional reactivity. Caudate volume correlated with IENFD, an indicator of small fiber degeneration.[75] Given that there were no correlations between IENFD and QST parameters, our findings suggest that peripheral degeneration and central sensory processing may be not necessarily linked to each other.[30] There are normative values for IENFD matched by area and sex. In this work, we used reference values from Lauria et al.[5] IENFD is a marker of peripheral nerve degeneration. Reduced IENFDs are therefore a typical sign of SFN, which is, however, unspecific to its etiology. Notably, none of the correlations survived Bonferroni correction for multiple testing. We reported the uncorrected results for caudate correlations only because GMV reduction in the caudate is the main finding of the study. Note that these correlations need to be interpreted with caution. However, the findings may potentially provide a basis for new hypotheses in future studies.

In patients, we identified reduced GMV in regions, for which volume reductions have already been reported in previous studies on chronic pain.[24-27] Reduced GMV might reflect an insufficient capacity in frontal pain modulatory network areas such as (m)SFG, MFG and IFG.[76] Volume reduction in frontal regions may point to deficient 'keeping pain out of mind'-functioning in chronic pain.[77]. Our finding is in line with previous research pointing to pain modulatory alterations in chronic pain patients.

We found decreased insula volume in patients. The insula is crucial for pain perception and chronification.[78] VBM studies provide evidence for decreased insula volume in several pain conditions.[58,60] We assume that reduced insula GMV does not reflect the cause of SFN, but rather a consequence of chronic nociceptive processing.[79] Ongoing pain, accompanied by behavioral impairment in form of reduced physical, social, and emotional performance,[80-82] may be reflected by reduced GMV.

We identified decreased CT for SFN patients in right PreCG. CT reduction was found in patients with- and without Nav variants pointing to robust deficits across patients. PreCG is relevant for integrating sensorimotor processes, for example, movement control.[83] Furthermore,

PreCG comprises primary motor cortex that is involved in pain modulation.[84] Reduced PreCG CT has been found in previous studies on chronic[29] and neuropathic pain[28] setting our result in line with previous research.

Limitations

The caudate nucleus was the only brain region identified by whole brain and region-based analysis indicating a robust finding. Therefore, remaining structural findings that have been identified by only one approach must be treated more cautiously. Restricted sample size and accompanied reduced statistical power is a concern, nevertheless the main analyses comprise more than 20 subjects in each group. With respect to partial correlation analyses it must be noted that several tests have been performed and none of the correlations survived corrections for multiple testing. Analyses on patients with rare Nav variants suffer from low statistical power because the subsample comprised 9 patients only. These variants are not proven pathogenic but 'only' variants of uncertain significance. Exploratory analyses need to be validated in larger samples before resilient conclusions are drawn from these preliminary results. Further, there is no gold standard for the diagnosis of SFN, meaning that criteria can never meet a sensitivity and specifity of 100%. In this cohort, however, we applied the established diagnostic algorithm[1] assessing a detailed plan and overall symptom history, excluding large fiber neuropathy by nerve conduction studies of both sensory and motor distal nerves, and then applied a detailed QST program plus skin biopsies in order to solidify the diagnosis. With this approach, we are as sure as can be that these patients all have SFN without exhibiting large fiber polyneuropathy at the time of examination. To make our data comparable to the published literature and reference data, we sticked to the DFNS QST protocol. It is a limitation of our study that we have used mainly static rather than dynamic evoked-pain measures to assess the performance of the somatosensory system of our SFN patients. Depressive mood or frequent use of pain medication and antidepressants must be considered as potential sources for alterations in brain tissue.[85] We excluded patients reporting depressive symptoms and calculated analyses again. For VBM, SBM, and region-based approach we identified the same regions as in the former analyses. We do not assume that medication intake accounts for structural changes observed between SFN patients and HC.

Conclusions

The present study shows GMV and CT changes in SFN patients. Most prominent is the volume reduction in SFN patients observed in left caudate, which was evident in voxel-based and region-based analyses and survived FDR correction. Behavioral analyses revealed that this region was associated with the behavioral category Reward suggesting GMV reductions may point to deficits in reward processing. The amount of this reduction was negatively correlated with patient's CPT and HPT, which may be related to their diminished ability to suppress pain. Additional studies are needed to prove this hypothesis. Likewise, the potential effect of genetic variants in Nav channels on GMV reductions has to be further validated. We also found some evidence that GMV reduction in caudate nucleus might be related to variants in genes associated with Nav channel functioning. These last 2 statements must be treated with care and await validation in future studies. Additionally, GMV reductions in SFN patients were observed in cortical regions like bilateral frontal cortex, right parietal lobule, and left insula. The latter findings are interpreted as a consequence of chronicized nociceptive processing. We assume GMV and CT alterations may provide a framework for future clinical research aiming to identify potential biological marker for SFN.

Disclosures

This work was funded by the Deutsche Forschungsgemeinschaft (DFG, German Research Foundation)—368482240/GRK2416 ('RTG 2416 MultiSenses—MultiScales'), by a grant from the Interdisciplinary Center for Clinical Research within the faculty of Medicine at the RWTH Aachen University (IZKF TN1-8/IA 532008, IZKF TN1-6/IA 532006, IZKF TN1-1/IA 532001, IZKF TN1-2/IA 532002, IZKF TN1-9/IA 532009) and the Brain Imaging Facility of the Interdisciplinary Center for Clinical Research (IZKF) within the faculty of Medicine at the RWTH Aachen University, Germany. This work was supported under the framework of international cooperation program managed by the National Research Foundation of Korea (2023K2A9A2A22000113).

The authors declare no conflicts of interest related to the present study.

Acknowledgments

Contributions that need acknowledging but do not justify authorship and acknowledgments: The authors would like to thank all volunteers for participation in our study. Further, we thank Timo Hottel, Leon Vangangelt, Max Röhl, and Sophie Schenk for their assistance during data collection. Moreover, we wish to thank Greta Peschke for providing support with data preparation before the analyses.

Appendix A. Supporting information

Supplementary data associated with this article can be found in the online version at doi:10.1016/j.jpain.2024.01.001.

References

1. Devigili G, Tugnoli V, Penza P, *et al.* The diagnostic criteria for small fibre neuropathy: from symptoms to neuropathology. Brain 131(7):1912-1925, 2008. https://doi.org/10.1093/brain/awn093

2. Sopacua M, Hoeijmakers JG, Merkies IS, Lauria G, Waxman SG, Faber CG: Small-fiber neuropathy: expanding the clinical pain universe. J Peripher Nerv Syst 24(1):19-33, 2019. https://doi.org/10.1111/jns.12298

3. Peters MJ, Bakkers M, Merkies IS, Hoeijmakers JG, van Raak EP, Faber CG: Incidence and prevalence of small-fiber neuropathy: a survey in the Netherlands. Neurology 81(15):1356-1360, 2013. https://doi.org/10.1212/wnl.0b013e3182a8236e

4. Hoitsma E, Drent M, Verstraete E, *et al.* Abnormal warm and cold sensation thresholds suggestive of small-fibre neuropathy in sarcoidosis. Clin Neurophysiol 114(12):2326-2333, 2003. https://doi.org/10.1016/s1388-2457(03)00259-1

5. Lauria G, Bakkers M, Schmitz C, *et al.* Intraepidermal nerve fiber density at the distal leg: a worldwide normative reference study. J Peripher Nerv Syst 15(3):202-207, 2010. https://doi.org/10.1111/j.1529-8027.2010.00271.x

6. Lauria G, Hsieh ST, Johansson O, *et al.* European Federation of Neurological Societies/Peripheral Nerve Society Guideline on the use of skin biopsy in the diagnosis of small fiber neuropathy. Report of a joint task force of the European Fe-deration of Neurological Societies and the Peripheral Nerve Society. Eur J Neurol 17(7):903-e49, 2010. https://doi.org/10.1111/j.1468-1331.2010.03023.x

7. Mendell JR, Sahenk Z: Painful sensory neuropathy. N Engl J Med 348(13):1243-1255, 2003. https://doi.org/10.1056/nejmcp022282

8. Tavee J, Zhou L: Small fiber neuropathy: a burning problem. Cleve Clin J Med 76(5):297-305, 2009. https://doi.org/10.3949/ccjm.76a.08070

9. Chao CC, Tseng MT, Lin YH, *et al.* Brain imaging signature of neuropathic pain phenotypes in small-fiber neuropathy: altered thalamic connectome and its associations with skin nerve degeneration. Pain 162(5):1387-1399, 2021. https://doi.org/10.1097/j.pain.0000000000002155

10. Hsieh PC, Tseng MT, Chao CC, *et al.* Imaging signatures of altered brain responses in small-fiber neuropathy: reduced functional connectivity of the limbic system after peripheral nerve degeneration. Pain 156(5):90, 2015. https://doi.org/10.1097/j.pain.0000000000000128

11. Tseng MT, Chiang MC, Chao CC, Tseng WYI, Hsieh ST: fMRI evidence of degeneration-induced neuropathic pain in diabetes: enhanced limbic and striatal activations. Hum Brain Mapp 34(10):2733-2746, 2013. https://doi.org/10.1002%2Fhbm.22105

12. Hansen TM, Muthulingam JA, Brock B, *et al.* Reduced gray matter brain volume and cortical thickness in adults with type 1 diabetes and neuropathy. Neurosci Res 176(2022):66-72, 2022. https://doi.org/10.1016/j.neures.2021.10.002

13. Selvarajah D, Wilkinson ID, Maxwell M, *et al.* Magnetic resonance neuroimaging study of brain structural differences in diabetic peripheral neuropathy. Diabetes Care 37(6):1681-1688, 2014. https://doi.org/10.2337/dc13-2610

14. Zhang Y, Qu M, Yi X, *et al.* Sensorimotor and pain-related alterations of the gray matter and white matter in Type 2 diabetic patients with peripheral neuropathy. Hum Brain Mapp 41(3):710-725, 2020. https://doi.org/10.1002%2Fhbm.24834

15. Bennett DL, Clark AJ, Huang J, Waxman SG, Dib-Hajj SD: The role of voltage-gated sodium channels in pain signaling. Physiol Rev 99(2):1079-1151, 2019. https://doi.org/10.1152/physrev.00052.2017

16. Faber CG, Hoeijmakers JG, Ahn HS, *et al.* Gain of function Nav1. 7 mutations in idiopathic small fiber neuropathy. Ann Neurol 71(1):26-39, 2012. https://doi.org/10.1002/ana.22485

17. Faber CG, Lauria G, Merkies IS, *et al.* Gain-of-function Nav1. 8 mutations in painful neuropathy. Proc Natl Acad Sci USA 109(47):19444-19449, 2012. https://doi.org/10.1073%2Fpnas.1216080109

18. Hoitsma E, Reulen JPH, De Baets M, Drent M, Spaans F, Faber CG: Small fiber neuropathy: a common and important clinical disorder. J Neurol Sci 227(1):119-130, 2004. https://doi.org/10.1016/j.jns.2004.08.012

19. Dib-Hajj SD, Yang Y, Black JA, Waxman SG: The NaV1. 7 sodium channel: from molecule to man. Nat Rev Neurosci 14(2013):49-62, 2013. https://doi.org/10.1038/nrn3404

20. Han C, Vasylyev D, Macala LJ, *et al.* The G1662S NaV1. 8 mutation in small fibre neuropathy: impaired inactivation underlying DRG neuron hyperexcitability. J Neurol Neurosurg Psychiatry 85(5):499-505, 2014. https://doi.org/10.1136/jnnp-2013-306095

21. Huang J, Yang Y, Zhao P, *et al.* Small-fiber neuropathy Nav1.8 mutation shifts activation to hyperpolarized potentials and increases excitability of dorsal root ganglion neurons. J Neurosci 33(35):14087-14097, 2013. https://doi.org/10.1523/jneurosci.2710-13.2013

22. Kaluza L, Meents JE, Hampl M, *et al.* Loss-of-function of Nav1. 8/D1639N linked to human pain can be rescued by lidocaine. Pflug Arch Eur J Phys 470(2018):1787-1801, 2018. https://doi.org/10.1007/s00424-018-2189-x

23. Lampert A, Eberhardt M, Waxman SG: Altered sodium channel gating as molecular basis for pain: contribution of activation, inactivation, and resurgent currents. Hand Exp Pharmacol 221(2014):91-110, 2014. https://doi.org/10.1007/978-3-642-41588-3_5

24. Henn AT, Larsen B, Frahm L, *et al.* Structural imaging studies of patients with chronic pain: an anatomic likelihood estimate meta-analysis. Pain 164(1):10-1097, 2022. https://doi.org/10.1097/j.pain.0000000000002681

25. Henssen D, Dijk J, Knepflé R, Sieffers M, Winter A, Vissers K: Alterations in grey matter density and functional connectivity in trigeminal neuropathic pain and trigeminal neuralgia: a systematic review and meta-analysis. NeuroImage Clin 24(2019):102039 https://doi.org/10.1016%2Fj.nicl.2019.102039

26. Pan PL, Zhong JG, Shang HF, *et al.* Quantitative meta-analysis of grey matter anomalies in neuropathic pain. Eur J Pain 19(9):1224-1231, 2015. https://doi.org/10.1002/ejp.670

27. Smallwood RF, Laird AR, Ramage AE, *et al.* Structural brain anomalies and chronic pain: a quantitative meta-analysis of gray matter volume. J Pain 14(7):663-675, 2013. https://doi.org/10.1016/j.jpain.2013.03.001

28. DaSilva AF, Becerra L, Pendse G, Chizh B, Tully S, Borsook D: Colocalized structural and functional changes in the cortex of patients with trigeminal neuropathic pain. PLoS One 3(10):e3396 https://doi.org/10.1371%2Fjournal.pone.0003396

29. Magon S, Sprenger T, Otti A, Papadopoulou A, Gündel H, Noll-Hussong M: Cortical thickness alterations in chronic pain disorder: an exploratory MRI study. Psychosom Med 80(7):592-598, 2018. https://doi.org/10.1097/psy.0000000000000605

30. Dohrn MF, Dumke C, Hornemann T, *et al.* Deoxysphingolipids, oxidative stress, and vitamin C correlate with qualitative and quantitative patterns of small fiber dysfunction and degeneration. Pain 163(9):1800-1811, 2022. https://doi.org/10.1097%2Fj.pain.0000000000002580

31. Rolke R, Baron R, Maier CA, *et al.* Quantitative sensory testing in the German Research Network on Neuropathic Pain (DFNS): standardized protocol and reference values. Pain 123(3):231-243, 2006. https://doi.org/10.1016/j.pain.2006.01.041

32. Rolke R, Magerl W, Campbell KA, *et al.* Quantitative sensory testing: a comprehensive protocol for clinical trials. Eur J Pain 10(1):77-88, 2006. https://doi.org/10.1016/j.ejpain.2005.02.003

33. Freynhagen R, Baron R, Gockel U, Tölle TR: Pain DETECT: a new screening questionnaire to identify neuropathic components in patients with back pain. Curr Med Res Opin 22(10):1911-1920, 2006. https://doi.org/10.1185/030079906×132488

34. Freynhagen R, Tölle TR, Gockel U, Baron R: The painDETECT project–far more than a screening tool on neuropathic pain. Curr Med Res Opin 32(6):1033-1057, 2016. https://doi.org/10.1185/03007995.2016.1157460

35. Hartrick CT, Kovan JP, Shapiro S: The numeric rating scale for clinical pain measurement: a ratio measure? Pain Pract 3(4):310-316, 2003. https://doi.org/10.1111/j.1530-7085.2003.03034.x

36. Krebs EE, Carey TS, Weinberger M: Accuracy of the pain numeric rating scale as a screening test in primary care. J Gen Intern Med 22(2007):1453-1458, 2007. https://doi.org/10.1007/s11606-007-0321-2

37. Williamson A, Hoggart B: Pain: a review of three commonly used pain rating scales. J Clin Nurs 14(7):798-804, 2005. https://doi.org/10.1111/j.1365-2702.2005.01121.x

38. Richards S, Aziz N, Bale S, *et al.* Standards and guidelines for the interpretation of sequence variants: a joint consensus recommendation of the American College of Medical Genetics and Genomics and the Association for Molecular Pathology. Genet Med 17(5):405-423, 2015. https://doi.org/10.1038/gim.2015.30

39. Gaser C, Dahnke R, Thompson PM, Kurth F, Luders E: CAT-a computational anatomy toolbox for the analysis of structural MRI data. BioRxiv :1-37, 2022. https://doi.org/10.1101/2022.06.11.495736

40. Ashburner J, Friston KJ: Voxel-based morphometry—the methods. NeuroImage 11(6):805-821, 2000. https://doi.org/10.1006/nimg.2000.0582

41. Coppola G, Petolicchio B, Di Renzo A, *et al.* Cerebral gray matter volume in patients with chronic migraine: correlations with clinical features. J Headache Pain 18(115):1-9, 2017. https://doi.org/10.1186%2Fs10194-017-0825-z

42. Weise CM, Bachmann T, Schroeter ML, Saur D: When less is more: structural correlates of core executive functions in young adults–a VBM and cortical thickness study. NeuroImage 189(2019):896-903, 2019. https://doi.org/10.1016/j.neuroimage.2019.01.070

43. Cauda F, Palermo S, Costa T, *et al.* Gray matter alterations in chronic pain: a network-oriented meta-analytic approach. NeuroImage Clin 4(2014):676-686, 2014. https://doi.org/10.1016/j.nicl.2014.04.007

44. Tatu K, Costa T, Nani A, *et al.* How do morphological alterations caused by chronic pain distribute across the brain? A meta-analytic co-alteration study. NeuroImage Clin 18(2018):15-30, 2018. https://doi.org/10.1016/j.nicl.2017.12.029

45. Yoon EJ, Kim YK, Shin HI, Lee Y, Kim SE: Cortical and white matter alterations in patients with neuropathic pain after spinal cord injury. Brain Res 1540(2013):64-73, 2013. https://doi.org/10.1016/j.brainres.2013.10.007

46. Benjamini Y, Hochberg Y: Controlling the false discovery rate: a practical and powerful approach to multiple testing. J R Stat Soc Ser B Stat Methodol 57(1):289-300, 1995.⟨https://www.jstor.org/stable/2346101⟩

47. Dahnke R, Yotter RA, Gaser C: Cortical thickness and central surface estimation. NeuroImage 65(15):336-348, 2013. https://doi.org/10.1016/j.neuroimage.2012.09.050

48. Yotter RA, Dahnke R, Thompson PM, Gaser C: Topological correction of brain surface meshes using spherical harmonics. Hum Brain Mapp 32(7):1109-1124, 2011. https://doi.org/10.1002/hbm.21095

49. Fischl B, Dale AM: Measuring the thickness of the human cerebral cortex from magnetic resonance images. Proc Natl Acad Sci USA 97(20):11050-11055, 2000. https://doi.org/10.1073/pnas.200033797

50. Kharabian Masouleh S, Eickhoff SB, Zeighami Y, *et al.* Influence of processing pipeline on cortical thickness measurement. Cereb Cortex 30(9):5014-5027, 2020. https://doi.org/10.1093/cercor/bhaa097

51. Yotter RA, Thompson PM, Gaser C: Algorithms to improve the reparameterization of spherical mappings of brain surface meshes. J. Neuroimaging 21(2):e134-e147, 2011. https://doi.org/10.1111/j.1552-6569.2010.00484.x

52. Barnes J, Ridgway GR, Bartlett J, *et al.* Head size, age and gender adjustment in MRI studies: a necessary nuisance? NeuroImage 53(4):1244-1255, 2010. https://doi.org/10.1016/j.neuroimage.2010.06.025

53. Destrieux C, Fischl B, Dale A, Halgren E: Automatic parcellation of human cortical gyri and sulci using standard anatomical nomenclature. NeuroImage 53(1):1-15, 2010. https://doi.org/10.1016/j.neuroimage.2010.06.010

54. Yeung AWK, Robertson M, Uecker A, Fox PT, Eickhoff SB: Trends in the sample size, statistics, and contributions to the BrainMap database of activation likelihood estimation meta-analyses: an empirical study of 10–year data. Hum Brain Mapp 44(5):1876-1887, 2023. https://doi.org/10.1002/hbm.26177

55. Eickhoff SB, Bzdok D, Laird AR, *et al.* Co-activation patterns distinguish cortical modules, their connectivity and functional differentiation. NeuroImage 57(3):938-949, 2011. https://doi.org/10.1016/j.neuroimage.2011.05.021

56. Lancaster JL, Laird AR, Eickhoff SB, Martinez MJ, Fox PM, Fox PT: Automated regional behavioral analysis for human brain images. Front Neuroinform 6(2012):23, 2012. https://doi.org/10.3389/fninf.2012.00023 1-12

57. Absinta M, Rocca MA, Colombo B, Falini A, Comi G, Filippi M: Selective decreased grey matter volume of the pain-matrix network in cluster headache. Cephalalgia 32(2):109-115, 2012. https://doi.org/10.1177/0333102411431334

58. Lan DY, Zhu PW, He Y, *et al.* Gray matter volume changes in patients with acute eye pain: a voxel-based morphometry study. Transl Vis Sci Technol 8(1):1-11, 2019. https://doi.org/10.1167/tvst.8.1.1

59. Li M, Yan J, Li S, *et al.* Reduced volume of gray matter in patients with trigeminal neuralgia. Brain Imaging Behav 11(2017):486-492, 2017. https://doi.org/10.1007/s11682-016-9529-2

60. Obermann M, Rodriguez-Raecke R, Naegel S, *et al.* Gray matter volume reduction reflects chronic pain in trigeminal neuralgia. NeuroImage 74(2013):352-358, 2013. https://doi.org/10.1016/j.neuroimage.2013.02.029

61. Becker S, Gandhi W, Schweinhardt P: Cerebral interactions of pain and reward and their relevance for chronic pain. Neurosci Lett 520(2):182-187, 2012. https://doi.org/10.1016/j.neulet.2012.03.013

62. Elvemo NA, Landrø NI, Borchgrevink PC, Håberg AK: Reward responsiveness in patients with chronic pain. Eur J Pain 19(10):1537-1543, 2015. https://doi.org/10.1002/ejp.687

63. Liu X, Wang N, Gu L, Guo J, Wang J, Luo F: Reward processing under chronic pain from the perspective of "liking" and "wanting": a narrative review. Pain Res Manag 2019:1-8, 2019. https://doi.org/10.1155%2F2019%2F6760121

64. Navratilova E, Morimura K, Xie JY, Atcherley CW, Ossipov MH, Porreca F: Positive emotions and brain reward circuits in chronic pain. J Comp Neurol 524(8):1646-1652, 2016. https://doi.org/10.1002%2Fcne.23968

65. Segerdahl AR, Xie J, Paterson K, Ramirez JD, Tracey I, Bennett DL: Imaging the neural correlates of neuropathic pain and pleasurable relief associated with inherited erythromelalgia in a single subject with quantitative arterial spin labelling. Pain 153(5):1122-1127, 2012. https://doi.org/10.1016/j.pain.2011.12.012

66. Meents JE, Bressan E, Sontag S, *et al.* The role of Nav1. 7 in human nociceptors: insights from human induced pluripotent stem cell–derived sensory neurons of erythromelalgia patients. Pain 160(6):1327-1341, 2019. https://doi.org/10.1097/j.pain.0000000000001511

67. Mis MA, Yang Y, Tanaka BS, *et al.* Resilience to pain: a peripheral component identified using induced pluripotent stem cells and dynamic clamp. J Neurosci 39(3):382-392, 2019. https://doi.org/10.1523/jneurosci.2433-18.2018

68. Namer B, Schmidt D, Eberhardt E, *et al.* Pain relief in a neuropathy patient by lacosamide: Proof of principle of clinical translation from patient-specific iPS cell-derived nociceptors. EBioMedicine 39:401-408, 2019. https://doi.org/10.1016/j.ebiom.2018.11.042

69. Freund W, Klug R, Weber F, Stuber G, Schmitz B, Wunderlich AP: Perception and suppression of thermally induced pain: a fMRI study. Somatosens. Mot. Res. 26(1):1-10, 2009. https://doi.org/10.1080/08990220902738243

70. Freund W, Stuber G, Wunderlich AP, Schmitz B: Cortical correlates of perception and suppression of electrically induced pain. Somatosens Mot Res 24(6):203-212, 2007. https://doi.org/10.1080/08990220701723636

71. Wunderlich AP, Klug R, Stuber G, Landwehrmeyer B, Weber F, Freund W: Caudate nucleus and insular activation during a pain suppression paradigm comparing thermal and electrical stimulation. Open Neuroimaging J 5(2011):1-8, 2011. https://doi.org/10.2174%2F1874440001105010001

72. Le Cann K, Meents JE, Sudha Bhagavath Eswaran V, *et al.* Assessing the impact of pain-linked Nav1.7 variants: an example of two variants with no biophysical effect. Channels 15(1):208-228, 2021. https://doi.org/10.1080/19336950.2020.1870087

73. Waxman SG, Merkies IS, Gerrits MM, *et al.* Sodium channel genes in pain-related disorders: phenotype–genotype associations and recommendations for clinical use. Lancet Neurol 13(11):1152-1160, 2014. https://doi.org/10.1016/s1474-4422(14)70150-4

74. Becerra L, Morris S, Bazes S, *et al.* Trigeminal neuropathic pain alters responses in CNS circuits to mechanical (brush) and thermal (cold and heat) stimuli. J Neurosci 26(42):10646-10657, 2006. https://doi.org/10.1523%2FJNEUROSCI.2305-06.2006

75. Pittenger GL, Ray M, Burcus NI, McNulty P, Basta B, Vinik AI: Intraepidermal nerve fibers are indicators of small-fiber neuropathy in both diabetic and nondiabetic patients. Diabetes Care 27(8):1974-1979, 2004. https://doi.org/10.2337/diacare.27.8.1974

76. Yang FC, Chou KH, Fuh JL, *et al.* Altered gray matter volume in the frontal pain modulation network in patients with cluster headache. Pain 154(6):801-807, 2013. https://doi.org/10.1016/j.pain.2013.02.005

77. Lorenz J, Minoshima S, Casey KL: Keeping pain out of mind: the role of the dorsolateral prefrontal cortex in pain modulation. Brain 126(5):1079-1091, 2003. https://doi.org/10.1093/brain/awg102

78. Lu C, Yang T, Zhao H, *et al.* Insular cortex is critical for the perception, modulation, and chronification of pain. Neurosci Bull 32(2016):191-201, 2016. https://doi.org/10.1007/s12264-016-0016-y

79. May A: Chronic pain may change the structure of the brain. Pain 137(1):7-15, 2008. https://doi.org/10.1016/j.pain.2008.02.034

80. Apkarian AV, Sosa Y, Krauss BR, *et al.* Chronic pain patients are impaired on an emotional decision-making task. Pain 108(1):129-136, 2004. https://doi.org/10.1016/j.pain.2003.12.015

81. Bryant LL, Grigsby J, Swenson C, Scarbro S, Baxter J: Chronic pain increases the risk of decreasing physical performance in older adults: the San Luis Valley Health and Aging Study. J Gerontol A Biol Sci Med Sci 62(9):989-996, 2007. https://doi.org/10.1093/gerona/62.9.989

82. Elman I, Zubieta JK, Borsook D: The missing p in psychiatric training: why it is important to teach pain to psychiatrists. Arch Gen Psychiatry 68(1):12-20, 2011. https://doi.org/10.1001%2Farchgenpsychiatry.2010.174

83. Cooke DF, Graziano MS: Sensorimotor integration in the precentral gyrus: polysensory neurons and defensive movements. J Neurophysiol 91(4):1648-1660, 2004. https://doi.org/10.1152/jn.00955.2003

84. Tracey I, Mantyh PW: The cerebral signature for pain perception and its modulation. Neuron 55(3):377-391, 2007. https://doi.org/10.1016/j.neuron.2007.07.012

85. Schmidt-Wilcke T: Variations in brain volume and regional morphology associated with chronic pain. Curr Rheumatol Rep 10(2008):467-474, 2008. https://doi.org/10.1007/s11926-008-0077-7